IEEE Transactions on Nuclear Science, Vol. NS-32, No. 5, October 1985

LANDAU DAMPING IN THE SLAC LINAC*

K. L. F. BANE

Stanford Linear Accelerator Center
Stanford University, Stanford, California, 94305

Introduction

In the SLC, after leaving its damping ring, the electron (or positron) bunch is accelerated from 1.2 GeV to 50 GeV in sectors 2-30 of the linac, before entering the collider arcs. It is important that the beam emittance growth in these sectors be small, since the luminosity depends inversely on the final emittance. For 5×10^{10} particles per bunch slight excursions from the structure axis will induce dipole wake forces that will tend to cause large emittance growth, also known as single bunch beam break-up. Position monitors and correctors are installed that will help keep the beam close to the structure axis. Further, instrumentation will be added that will allow the initial x, x', y, y' of the beam to be varied, to compensate coherent effects of machine errors,[1] until the best quality beam reaches the end of the linac. These measures, however, will have no effect on the pulse-to-pulse jitter of injection, whose tolerances turn out to be quite stringent in the SLC. According to calculations,[2] the allowable jitter amounts to 1% of σ_{x0} positional and 1% of $\sigma_{x'0}$ angular injection errors, either of which results in an emittance growth of 25%.

In the SLC the beam leaves the damping ring with very little energy spread. Following an idea used in the VLEPP design,[3] we propose running the bunch behind the crest of the RF wave in the early part of the linac, in order to induce a large coherent energy spread between the head and the tail of the bunch. This energy spread induces a damping similar to Landau damping that stabilizes the beam against the large transverse wakefields. This extra energy spread is gradually removed by placing the bunch at a suitable position in front of the crest of the RF wave in the later part of the linac. We shall see that this phase juggling results in greatly relaxed injection jitter tolerances, but at the cost of some final energy.

The Two-Particle Model

The two-particle model is a useful model for studying single bunch beam break-up in a linac[4,5] and the effect of Landau damping. Though somewhat crude, it displays the general features of the beam behaviour. Let the beam be modelled by two particles, each of charge $Q/2$ separated by a longitudinal distance z. For simplicity we let the energy of the two particles be constant, and we assume smooth focusing. The two particles have respectively wave numbers k, $k + \Delta k$, and energies E, $E + \Delta E$. Particle 1 feels no transverse wake force, and it undergoes free betatron oscillation. Particle 2, though, experiences the force $F_x = eQW_x(z)x_1/2$ due to the leading particle's motion, where $W_x(z)$ is the value of the dipole wake function for longitudinal separation z and x_1 is the transverse position of particle 1. Its equation of motion is that of a simple driven harmonic oscillator

$$x_2'' + (k + \Delta k)^2 x_2 = C x_1 \qquad (1)$$

where the independent variable is s the position along the machine and where $C = eQW_x(z)/2E$ for $|\Delta E/E|$ small.

Effective emittance growth is modelled here by the displacement of the particles in phase space. Hence we would like to keep the quantities $|x_2 - x_1|$ and $|x_2' - x_1'|$ small. If both particles have the same initial conditions and $\Delta k = 0$ then

$$\frac{(x_2 - x_1)}{\hat{x}} = \frac{iCs}{2k} e^{iks} , \qquad (2)$$

where $\hat{x}$ is a complex constant determined by the initial conditions. Eq. (2) is a linearly growing oscillation. The quantity $(x_2' - x_1')$ is just the derivative of Eq. (2) and would therefore also be represented by a linearly growing oscillation, for large s. For small $|\Delta k/k|$ but with $\Delta k \neq 0$ we get

$$\frac{(x_2 - x_1)}{\hat{x}} = \left(1 - \frac{C}{2k\Delta k}\right) 2i \sin\left(\frac{\Delta k\, s}{2}\right) e^{i(k + \frac{\Delta k}{2})s} . \qquad (3)$$

Eq. (3) represents two beating sine waves with amplitude $A = 2(1 - C/2k\Delta k)$. Here we easily see the asymmetry in the effectiveness of the damping. For least growth, that is, to minimize A, we want $\Delta k > 0$: the trailing particle should have lower energy than the leading particle, since the chromaticity $\xi < 0$ in a linac. In particular, if $A = 0$, that is if

$$\Delta E = \frac{eQW_x(z)}{4k^2\xi} , \qquad (4)$$

the trailing particle also undergoes pure betatron motion and exactly tracks the motion of the leading particle. (A similar relation is found in Ref. 3.) In this case the extra phase advance of Particle 2 over a given distance exactly cancels the wakefield kick it feels due to Particle 1. There is no emittance growth. For example, in the SLC, taking $z = 2\sigma_z = 2$mm, $Q = 5 \times 10^{10}e$, $W_x(z) = 2.4 \times 10^3$ V/pC/m^2,[6] and (with 90° phase advance per cell) $k = 2\pi/100$m, $\xi = -4/\pi$, the optimal energy spread would be $\Delta E \approx -1.0$GeV. This value is very large. By using stronger focusing, therefore increasing k, the optimal energy spread could be reduced.

We also note that both Eq. (3) and its derivative reach approximately zero for $\Delta k\, s/2 = n\pi$, where n is an integer. By a proper choice of Δk, one of these minima can be made to coincide with the end of the linac, thus minimizing the emittance there. We will exploit this property in maximizing the effectiveness of the damping in the linac of the SLC. For the first beat minimum to land at the end of the linac, where $s \approx 3000$m, requires that $< \Delta k > \approx 2 \times 10^{-3}$/m, where the brackets mean the average over the length of the machine. For the lattice described in the following section this roughly corresponds to an energy separation of the two particles of $\Delta E \approx -0.4$GeV.

The two-particle model can be simply extended by letting the two particles become two rigid longitudinal charge distributions. For two uniform distributions of charge, assuming Δk and W_x vary linearly with z, we still find the beating sine waves, although now the beat minima do not reach zero. We shall also see this property in the simulations. The model can be extended to include the effects of acceleration. Roughly all position and angular values will then be modified by the multiplicative factor $1/\sqrt{E_0 + Gs}$ where E_0 is the initial energy and G is the energy gradient.

The Simulation Program

Ref. 7 describes a method of tracking the bunch behaviour in a linac, including wakefields. The computer code LTRACK, which employs this method, divides a bunch into a number of slices longitudinally. It transports each slice's centroid and σ matrix through a lattice to first order by matrix multiplication.

* Work supported by the US Department of Energy, contract DE – AC03 – 76SF00515.

0018-9499/85/1000-2389$01.00© 1985 IEEE

In addition, when traversing a cavity, each slice is affected by the wakefields of the slices in front of it. For the simulations discussed here LTRACK has consulted a table of the longitudinal and dipole wakefields for the SLAC linac structure.[6]

We define here the total effective x-emittance of a bunch

$$\epsilon_x^2 = \sigma_{xx}\sigma_{x'x'} - \sigma_{xx'}^2 \ , \tag{5}$$

where

$$\sigma_{xx} = \frac{1}{Q}\sum_{i=1}^{M} Q_i \bar{\sigma}_{xxi} \ , \tag{6}$$

Q is the total charge and M is the number of slices in the bunch, Q_i is the charge of slice i and $\bar{\sigma}_{xxi}$ is the square of the standard deviation in x of slice i about the centroid of the bunch. The other total moments $\sigma_{x'x'}$ and $\sigma_{xx'}$ are defined in an analogous fashion. We then define the emittance growth factor $\delta_{\epsilon x}$ from position 0 to position 1 in the linac as

$$\delta_{\epsilon x} = \frac{(\bar{\gamma}\epsilon_x)_1 - (\bar{\gamma}\epsilon_x)_0}{(\bar{\gamma}\epsilon_x)_0} \ , \tag{7}$$

where $\bar{\gamma}$ is the average energy of the bunch. Normally position 0 is taken to be the beginning and position 1 the end of the linac. Note that in beam break-up the invariant emittance of no slice ever changes. The effective emittance growth is due to the misalignment of the slice centroids in phase space.

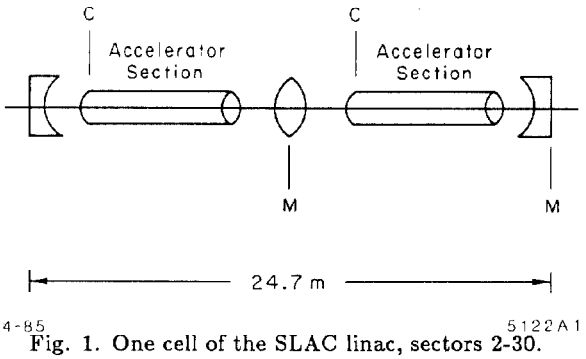

Fig. 1. One cell of the SLAC linac, sectors 2-30.

The layout of one cell of the SLAC linac, sectors 2-30 is shown schematically in Fig. 1. Four cells followed by a drift of 2.5 m make up one 100 meter sector. The peak accelerating gradient is 18 MeV/m. To induce an energy spread in the beam we separate the 232 klystrons (one for each 12 meter accelerator section) into two families. Family a contains n_a klystrons phased so that the bunch center sits at phase ϕ_a with respect to the RF crest. In family b, containing the remaining klystrons, the bunch sits at phase ϕ_b. In th SLC without Landau damping, for minimal energy spread at the end of the linac, the bunch needs to sit at 12° ahead of the RF crest, to compensate the variation of the longitudinal wakefield along the bunch.[2] With Landau damping, the bunch needs to see, on average, the same slope of the RF wave. Therefore, since all the accelerator sections are of the same length, we want

$$n_a \sin\phi_a + (232 - n_a)\sin\phi_b = 232 \sin 12° \ . \tag{8}$$

In all runs presented here the longitudinal distribution of the bunch is taken to be Gaussian, truncated from $4\sigma_z$ in front of bunch center to $2\sigma_z$ behind, and with σ_z = 1mm. The number of particles contained in a bunch is 5×10^{10}. The number of slices is 16. The initial normalized emittance is $\gamma\epsilon_x = 3.0 \times 10^{-5}$rm. All slices begin upright, with $\sigma_{x0} = 300\mu$m, $\sigma_{x'0} = 42\mu$r and energy E_0 = 1.21GeV. In all runs the quads are adjusted such that the β-function of the central slice is matched, and as given in Fig. 2. For the first 1300 m the phase advance per cell is 90°. From there to the end of the linac the quad strengths are approximately equal to 110 kilogauss, their maximal value.

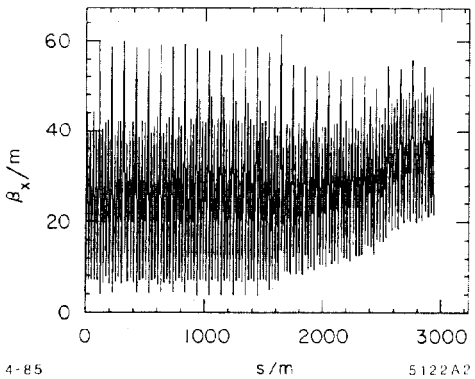

Fig. 2. The matched β-function in sectors 2-30.

The Ideal Machine

The LTRACK results for the SLAC linac with no errors are given in Fig. 3. Cases with $\phi_a = -15°, -30°, -45°, -60°$ were run. Fig. 3a gives the initial x offset that produces 25% emittance growth in the linac, x_d. The number n_a was adjusted in each case to maximize x_d. For the case with no Landau damping (denoted by NL in Fig. 3) we get $x_d = 2.1\mu$m. Fig. 3b gives the final energy E_F of the beam for the same runs. For no Landau damping E_F = 50.0GeV. The dashed curve gives E_F if we allow x_d to decrease by 20% from the optimal values, by reducing n_a, and gives an indication of the width of the minimum as a function of energy. We see that although we have more stability as ϕ_a becomes more negative (up to $\phi_a \approx -50°$) we lose more energy. The drop in x_d for $\phi_a < -50°$ is due to increased mismatch along the bunch (see below).

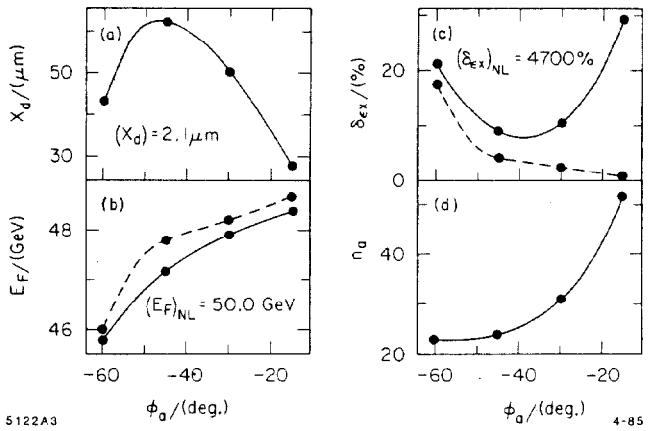

Fig. 3. Results for the error-free machine.

Fig. 3c gives the emittance growth for an initial offset $x_0 = 0.1\sigma_{x0} = 30\mu$m. For no Landau damping $\delta_{\epsilon x} = 4700\%$. The dashed curve is the emittance growth for a beam launched on axis, and is due only to the twisting of the slices with respect to one another in phase space. This effect is stronger for ϕ_a more negative, and is in fact the dominant effect for $\phi_a = -60°$. This is due to the greater lattice mismatch along the bunch when the energy spread is added quickly rather than more gradually along the linac. Fig. 3d gives the values of n_a used.

In Fig. 4 the beam behaviour with no Landau damping (column 1) is compared with the case where $\phi_a = -30°$ and $n_a = 31$ (column 2). The initial offset x_0 is 30μm. The bunch centroid $\bar{x}$ is plotted as a function of s in Fig. 4a, for the case with no damping. In Fig. 4b we see the rapid emittance growth along the linac. A scatter plot of the beam at the end of the linac is given in Fig. 4c. (The head is to the right.) Note that the tail half of the bunch is strongly perturbed; in comparison, the front half is little affected. For the case with damping the

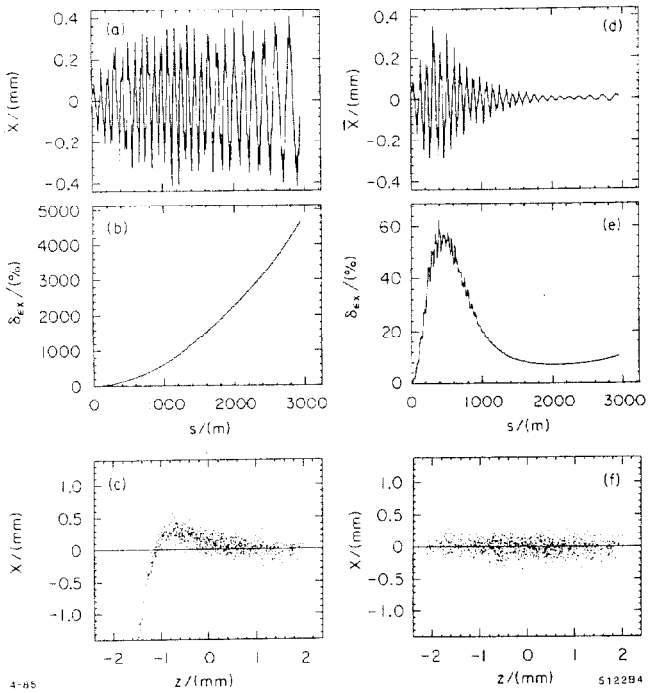

Fig. 4. Results without/with Landau damping.

beating effect is clearly evident in Fig. 4d, as is the well placed envelope minumum. A coherent emittance growth is induced early in the linac, which then largely disappears toward the end of the machine, as is seen in Fig. 4e. The beam arrives at the end of the linac relatively unperturbed, as shown in Fig. 4d.

The Machine With Errors

In order to study the effects of machine errors, runs with 100μm rms quadrupole offset errors (the SLC spec[2]) were done. Table 1 gives the results. Case 12 is with no Landau damping. In case 15 $\phi_a = -15°$ and $n_a = 51$; in case 30 $\phi_a = -30°$ and $n_a = 31$. The letters A-E represent four different sets of random numbers. First, correctors (C) were adjusted to correct a low current beam to beam position monitors (M) with 100μm rms offset errors (see Fig. 1). Then the high current beam was launched on axis with these same corrector settings. In this way the head of the beam was corrected to the monitors. (Correcting the high current beam directly does not work due to the large tail that is formed on the uncorrected beam with the level of errors studied here.) Column 2 gives the resultant emittance growth. The emittance growth at this point is much larger without than with Landau damping. By adjusting x_0 and x_0' coherent effects of the errors can be largely compensated (column 3). (In practise a screen monitor at the end of the linac would be used for the feedback in this procedure.) Note that the compensation is not perfect. In some cases the injection conditions have not enough leverage to reduce the final emittance to a small value. Note also that at this point Landau damping usually but not always results in a lower emittance growth than with no damping.

By adjusting two correctors which are 90° apart at the beginning of sector 6, we can reduce the emittance further (column 4). (In practise the screen monitor would again be used here.) At this point $\delta_{\epsilon x}$ is no bigger than 30% in all the Landau damped cases. With no Landau damping the extra correction has little effect. The final column gives the minimal change in x_0 that increases the emittance by 25% above the values given in column 4, Δx_d. (Normally the effect is not the same for equal changes in the two directions.) The results agree well with those for the error-free machine, ranging from

Case	$(\delta_{\epsilon x})_a$/%	$(\delta_{\epsilon x})_b$/%	$(\delta_{\epsilon x})_c$/%	$\Delta x_d/\mu$m
12A	944.	69.0	64.4	1.5
12B	1010.	39.9	37.5	1.8
12C	8150.	32.4	30.1	1.7
12D	3870.	404.2	374.6	2.6
12E	5080.	115.9	105.5	2.0
15A	271.	38.9	25.1	20.
15B	112.	10.3	6.9	24.
15C	82.	4.5	3.6	23.
15D	51.	16.7	11.4	20.
15E	332.	48.2	30.1	25.
30A	305.	126.2	23.5	36.
30B	92.	33.9	10.8	42.
30C	22.	6.0	4.7	51.
30D	138.	62.6	29.0	33.
30E	266.	96.1	18.7	39.

Table 1. Results for the machine with errors.

70-100% of the values given in Fig. 3a. These runs are a sort of proof of principle indicating that the dispersive effects are manageable, at least for ϕ_a down to $-30°$.

Conclusions

In the SLC Landau damping can greatly stabilize the beam against changes in injection conditions into the linac. For example, by choosing $\phi_a = -15°$, $n_a = 51$, the jitter tolerances for 25% emittance growth can be relaxed by greater than a factor of 10, while sacrificing 1.6 GeV in final energy. Increasing the focusing, especially near the beginning of the linac, will lessen the energy penalty for a given amount of stability. For example, with the planned addition of more quads in sectors 2-4[8] the stability of the above example can be achieved at the cost of only 1.0 GeV in final energy.[9] The simulations including machine errors indicate that the static residual emittance growth can be kept consistently below 30% with Landau damping, but that this would be difficult to achieve without Landau damping. It can be supposed that Landau damping will also stabilize the beam to magnet jitter, though a more thorough study of machine error effects still needs to be done.

Acknowledgements

The author greatly thanks A. Chao for his help and J. Seeman, J. Sheppard, R. Stiening for many discussions we have had. J. Sheppard supplied the matched lattice for Fig. 2.

References

[1] A. Chao, B. Richter, C. Yao, Nuclear Instruments and Methods **178**, 1 (1980).
[2] SLAC Linear Collider Conceptual Design Report, SLAC Report 229, (1980).
[3] V. Balakin, *et. al.*, Proceedings of the 12th Int. Conf. on High Energy Accelerators Fermilab, (1983), p. 119.
[4] P. Wilson in *Physics of High Energy Particle Accelerators*, AIP Conf. Proc. No. 87, (Am. Inst. of Physics, New York, 1982), Sec. 11.1.
[5] A. Chao in *Physics of High Energy Particle Accelerators*, AIP Conf. Proc. No. 105, (Am. Inst. of Physics, New York, 1983), Sec. 2.3.
[6] K. Bane and P. Wilson, Proceedings of the 11th Int. Conf. on High-Energy Accelerators, CERN (Birkhäuser Verlag, Basel, 1980), p. 592.
[7] A. Chao and R. Cooper, Particle Accelerators **13**, 1 (1983).
[8] J. Seeman, *et. al.* 'Observations of Accelerated High Current – Low Emittance Beams in the SLC Linac', This conference.
[9] K. Bane, to be published.